CIRP Annals - Manufacturing Technology 61 (2012) 107–110

Contents lists available at SciVerse ScienceDirect

CIRP Annals - Manufacturing Technology

journal homepage: http://ees.elsevier.com/cirp/default.asp

An energy based analysis of broaching operation: Cutting forces and resultant surface integrity

Hossam A. Kishawy (2)[a,*], Ali Hosseini [a], Behnam Moetakef-Imani [b], Viktor P. Astakhov [c]

[a] Machining Research Laboratory (MRL), Faculty of Engineering and Applied Science, University of Ontario Institute of Technology (UOIT), Oshawa, Ontario, Canada
[b] Department of Mechanical Engineering, Ferdowsi University of Mashhad, Mashhad, Iran
[c] General Motors Business Unit of Production Services Management, Saline, MI, USA

ARTICLE INFO

Keywords:
Cutting
Surface integrity
Broaching

ABSTRACT

As a single-pass machining operation, broaching is extensively used to produce simple and complicated profiles. Since a typical broaching tool includes roughing, semi-finishing and finishing teeth, its impact on the surface integrity is of prime interest. This paper presents an energy based analysis of the mechanics of cutting and the effects of successive teeth on the integrity of the machined surface. A cutting force model was developed and its authenticity was verified using the measured forces. The machined surfaces were used to study the effects of successive teeth on subsurface microhardness and subsurface microstructure.

1. Introduction

In industry, jobs such as design, optimization and reduction of the direct manufacturing costs associated with cutting tools are never-ending. These jobs are accomplished by the implementation of advanced cutting tools, which allows higher material removal rates. They are also accomplished by high-productivity manufacturing lines and cells, which are enhanced by intelligent process controllers. Furthermore, the jobs are achieved by improving the quality and reliability of machining operations. In doing such jobs, the structure of the direct tooling costs and their components must be thoroughly analysed to understand any possibility for cost reduction.

Tool manufacturers and specialists realized that the direct tooling cost associated with high-speed steel (HSS) tools may well exceed 50% in a modern automotive powertrain plant if it produces the full set of gears for transmissions. Moreover, 80% of the direct tooling cost of HSS tools are related to helical and spline broaches so that the direct tooling cost associated with HSS broaches is enormous (Fig. 1). Surprisingly, few research activities on HSS tools have been carried out over the last twenty years, specifically for broaching operation and tools [1–4]. No significant advances were made since the 1970s when powder metallurgy (PM) HSS was introduced. This is because of the common perception that HSS is an obsolete tool material (known since the end of the 19th century), which should have been substituted by more advanced tool materials a long time ago. Reality, however, shows otherwise, as HSS possesses a unique combination of properties (primarily hardness and toughness), which are essential for complex gear manufacturing tools. Compared to any other cutting tools, HSS broaches are highly productive and precise tools that meet the requirements of the cycle time in mass production such as in the automotive industry. In addition, it meets the requirements for high precision in the power and aerospace industries where slots for blades in the turbine disk are made using the so-called Christmas tree broaches.

Another important feature of HSS form broaches is their relatively low reliability that often makes broaching a bottle-neck operation in many modern powertrain plants. Generally, the low reliability of broaching operations is due to the absence of research on the design and geometry of such complex tools in spite of the fact that broaching tools and operations are:

1. The most expensive and one of the most complex tools in the automotive industry that accounts for the significant tooling cost.
2. Often producing the final surfaces to be used in service, i.e. directly responsible for quality and reliability of the product. And
3. Often bottle-neck operations due to low reliability of broaching tools.

The objective of this paper is to address two important issues in the analysis of the broaching process: first, it aims to develop an energy based force model to be used for any kind of broaching tools; second, it studies the depth of cold-working imposed by a broaching tool. The force model will be utilized in the design and geometrical optimization of the broaching tools as well as the broaching machines and desired fixtures for high precision requirements of broached parts. The depth of cold-working, in spline broaching of automotive components such as sun gears, is important since this operation is a finishing operation and thus directly determines the nose and reliability of the whole transmission. Moreover, because sun gears are subjected to heat treatment after broaching, the depth of cold-working determines the distortion due to the heat treatment. Therefore, the heat treatment regime should be adjusted correspondingly knowing this depth.

* Corresponding author.
E-mail address: hossam.kishawy@uoit.ca (H.A. Kishawy).

0007-8506/$ – see front matter © 2012 CIRP.
http://dx.doi.org/10.1016/j.cirp.2012.03.004

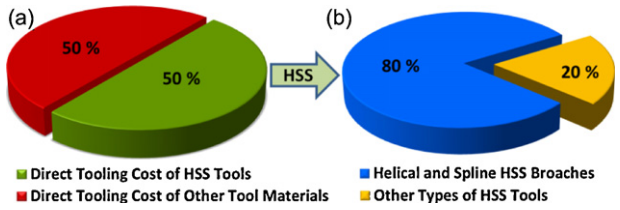

Fig. 1. Percentage of direct tooling cost for (a) HSS tools vs. other types of tool materials and (b) HSS helical and spline broaches vs. other types of HSS tools. (Courtesy of the General Motors Business Unit of Production Services Management.)

The result of the presented paper can be effectively applied to simulate, analyse and optimize any broaching tool in order to increase its efficiency and to decrease the tool manufacturing costs.

2. Energy based cutting force modelling

In an attempt to quantify the cutting force (the component of force along the cutting velocity) in a cutting system as a function of different power components spent during the process, the following formula was proposed [5].

$$F_c = \frac{P_c}{v} = \frac{P_{fR} + P_{fF} + P_{pd} + P_{ch} + P_{mn-ce}}{v} \quad (1)$$

In Eq. (1), P_{fR} is the power consumed at the tool–chip interface; P_{fF} is the power consumed at the tool–workpiece interface; P_{pd} is the power spent on the plastic deformation of the removed layer by cutting tool; P_{ch} is the power consumed in the formation of new surfaces; and $P_{mn\text{-}ce}$ is the energy spent due to the combined influence of the minor cutting edge. In order to predict the cutting force in the broaching operation, each of the above mentioned components of cutting power must be accurately identified.

2.1. Friction at the tool–chip interface

The power spent at the tool–chip interface due to friction between tool and chip on the rake face can be calculated as [5]:

$$P_{fR} = \tau_c \times l_c \times b_{1T} \times \frac{v}{\xi} \quad \text{where} \quad \tau_c = 0.28 \times \sigma_R \quad (2)$$

$$l_c = t_{1T} \times \xi^k \quad (3)$$

where τ_c (N/m^2) is the average shear stress at the tool–chip interface, σ_R is the ultimate tensile strength of the workpiece material (N/m^2), b_{1T} is the true chip width (m) and v is cutting velocity (m/s). The tool–chip contact length l_c is calculated based on Eq. (3) where t_{1T} is the true uncut chip thickness (m) (rise per tooth), ξ is the chip compression ratio, and $k = 1.5$ when $\xi < 4$ and $k = 1.3$ when $\xi \geq 4$.

2.2. Friction at the tool–workpiece interface

The power spent because of friction at the tool–workpiece interface is calculated by the following equation:

$$P_{fF} = F_{fF} \times v_1 \quad \text{where} \quad v_1 = \frac{v}{\xi} \quad (4)$$

In Eq. (4), v_1 is the velocity of the chip and F_{fF} is the friction force on the tool–workpiece interface.

$$F_{fF} = 0.625 \times \tau_y \times \rho_{ce} \times l_{ac} \times \sqrt{\frac{B_r}{\sin\alpha}} \quad (5)$$

$$B_r = \frac{\cos\gamma}{\xi - \sin\gamma} \quad (6)$$

In Eq. (6), B_r is the Briks similarity criterion [6], τ_y is the shear strength of the workpiece material (N/m^2), ρ_{ce} is the radius of the cutting edge (m), α is the normal flank angle (deg), γ is the normal rake angle (deg), l_{ac} is the length of the active part of the cutting edge (the length of the edge engaged in cutting) (m).

2.3. Power spent on plastic deformation zone

This component of cutting power is calculated as follows:

$$P_{pd} = \frac{K(1.15 \times \ln\xi)^{n+1}}{n+1} \times v \times A_w \quad (7)$$

where K is the strength coefficient (N/m^2), n is the hardening exponent of the work material, A_w is uncut chip cross-sectional area (m^2). K and n are usually determined using engineering stress–strain curve by assuming negligible volume change. The most common mathematical formula that relates the true stress to true strain is a power expression as presented in Eq. (8) where, K is the stress at $\varepsilon_T = 1$ and n is the slope of a log–log plot of Eq. (8). It must be noted that Eq. (8) is valid before necking occurs [7].

$$\sigma_T = K \times (\varepsilon_T)^n \quad (8)$$

2.4. Formation of new surface and influence of minor cutting edge

The power spent due to formation of new surfaces (P_{ch}) is negligible in broaching as the cutting speed, and thus the frequency of chip formation is small. The energy spent due to the influence of the minor cutting edge ($P_{mn\text{-}ce}$) is assumed to be zero because broaching tool does not have minor cutting edge.

3. Force model verification

3.1. Mechanical properties of workpiece materials

Four different engineering materials were utilized in this study and standard tensile tests were carried out to obtain the required mechanical parameters. Table 1 shows the mechanical properties and the other required parameters for workpiece materials.

3.2. Experimental setup and test configuration

A broaching machine with 5000 kg maximum pull load capacity and 1000 mm maximum length of stroke was utilized to perform the cutting tests. A number of continuous and interrupted broaching tests were conducted on different workpiece materials to validate the model and to investigate the effects of broaching operation on the surface integrity of the machined surface. The generated cutting forces were measured using a KISTLER 9255b table dynamometer equipped with a 5070 charge amplifier. The broaching tool was digitized by RENISHAW Cyclone digitizer with 1 μm accuracy and the obtained set of data was used to extract the geometric features of cutting edges. The edge radius value has been also computed by circular regression of data points around the edge based on the method explained in [9]. Table 2 and Fig. 2 illustrate the geometrical features of the utilized broaching tool and the configuration of the experimental setup.

In the simulations, the cutting operation is assumed to be plain strain; therefore, the difference between the chip width before and after cutting is negligible. As a result, b_{1T} is equal to the length of

Table 1
Mechanical properties of the workpiece materials.

	AISI 1045	AISI 12L14	Al 7075	Brass
E (Mpa)	210	200	64	80
σ_{yield} (Mpa)	346	397	135	147
$\sigma_{R(ultimate)}$ (Mpa)	605	663	280	356
K (Gpa)	0.96	1.07	0.45	0.54
n	0.17	0.18	0.24	0.30
ξ	9	5	6	4
τ_y (Mpa)[8]	0.75 σ_R	0.75 σ_R	0.65 σ_R	0.65 σ_R
τ_c (Mpa)	169	186	78	100

Table 2
Specification of the utilized broaching tool.

Tool type	Full form-pull end
Minor diameter	23 mm
Number of splines on each tooth	10
Spline width	3.91 mm
Number of teeth	44
Rise per tooth	0.03 mm
Pitch	10 mm
Edge radius	5 μm
Length of broach	965.2 mm
Distance to first tooth	304.8 mm
Tool material	HSS (ASP2023)
Cutting velocity	1 m/min

the cutting edge ($l_{ac} = b_{1T} = 3.91$ mm). The true uncut chip thickness, t_{1T}, is also assumed to be equal to the difference between the heights of two successive cutting edges (t_{1T} = rise per tooth = 0.03 mm). The total force is calculated by multiplying the force per tooth calculated using Eq. (1) by the number of splines on each tooth and then by the number of teeth simultaneously engaged with the workpiece.

The simulated cutting force has been plotted versus measured forces in Fig. 3. As it can be seen, once the tool engages with the workpiece, the cutting force increases progressively until the maximum possible number of teeth is in engagement. Then, the cutting force oscillates between its maximum and minimum during the stable phase of cutting. Once the last tooth engages with the workpiece, the cutting force gradually drops as the tool leaves the workpiece. Fig. 3 verifies the agreement between the simulated and the measured data.

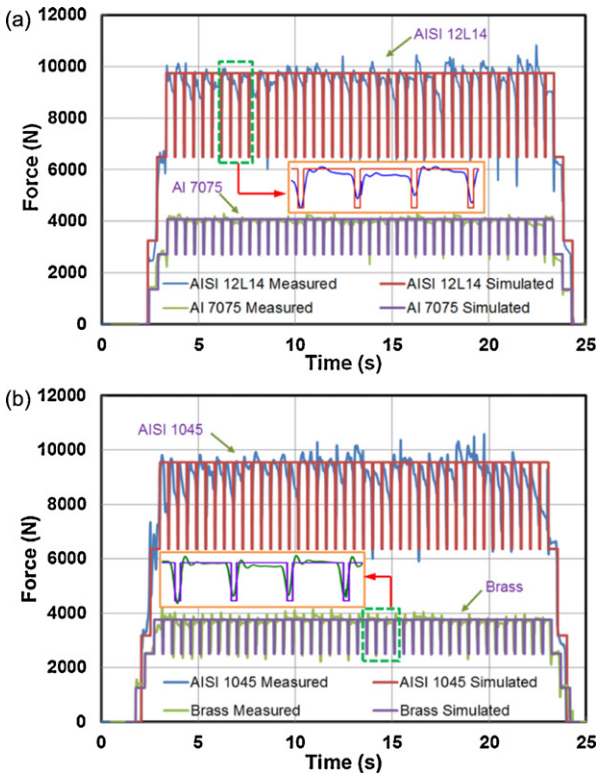

Fig. 3. Simulated and measured cutting force for (a) AISI 12L14 and Al 7075 and (b) AISI 1045 and brass.

4. Effects of broaching on subsurface microhardness

Small samples from the workpiece were prepared to investigate the effects of the broaching operation on the integrity of the machined surface. The samples were removed from the workpiece body using wire EDM to minimize the effects of the removal process on the surface integrity. The investigated integrity parameters are subsurface microhardness and subsurface microstructure. In interrupted cutting tests, the cutting tool was stopped at the middle of the cut, and it was retracted slowly. Due to the conical shape of the broaching tool, slow retraction of the tool does not damage the surface. Fig. 4 shows the mechanism of the test and the geometry of samples used for the surface integrity investigations.

The Vickers hardness (HV) method was utilized for measuring the microhardness beneath the broached surface. It has been clearly demonstrated by Fig. 5 that broaching operation aggressively changes the microhardness of the subsurface layers.

Fig. 5(a) and (b) show the microhardness beneath the broached surface for brass and steel AISI 12L14 for interrupted cut and full cut respectively. Each point represents the average of five data points which are measured at different locations along the same depth beneath the surface. As it can be seen, although successive teeth introduce more plastic deformation which is demonstrated by the higher microhardness reading, the depth of the plastically deformed layer was kept unchanged. Moreover, because the microhardness of the work material is uniquely related to the shear flow stress [6], the data obtained were used to calibrate the force model as the shear flow stress of the original work material is modified by Eq. (9) that accounts for the increase of the cutting force due to cold-working of the work material.

$$\sigma_{xy-fl} = 0.185\,\mathrm{HV} \tag{9}$$

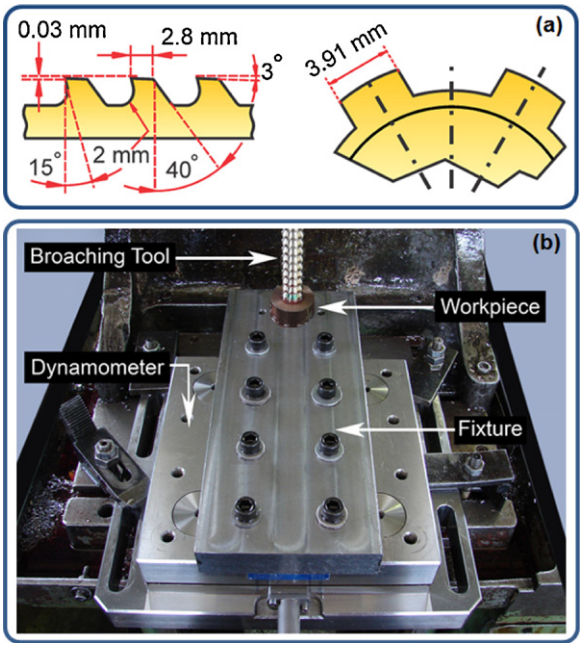

Fig. 2. (a) Geometry of the broaching tool, (b) Experimental setup.

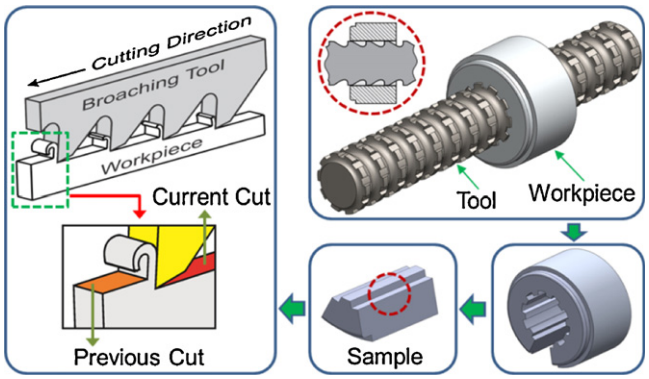

Fig. 4. Interrupted cutting and geometry of prepared sample.

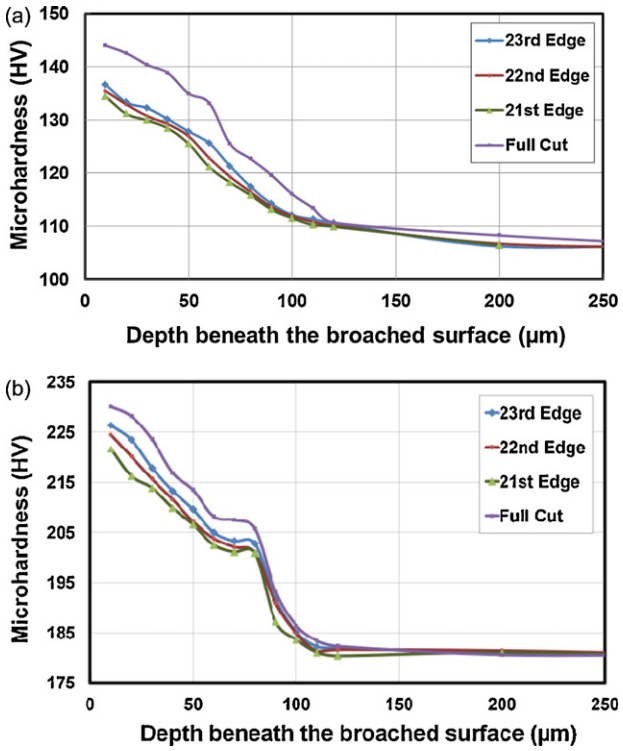

Fig. 5. Variation of microhardness beneath the broached surface: (a) Brass (b) AISI 12L14.

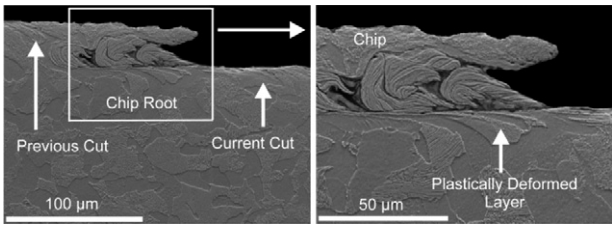

Fig. 6. SEM Image for the steel AISI 12L14 subsurface around the chip root for 23rd edge.

Since the depot of cold-working determined by the data shown in Fig. 5 (~70 μm) is greater than the rise per tooth (0.03 mm = 30 μm), each successive tooth of the broaching tool cuts the cold-worked layer.

5. Effects of broaching on subsurface microstructure

The magnitude of cutting forces in broaching is comparatively higher than that in other machining operations for the same uncut chip thickness. As a result, the depth of cold-working is relatively larger as can be seen in Fig. 5. To verify the findings shown in Fig. 5, SEM examination of the depth of cold-working and severity of the grain deformation were carried out. Fig. 6 shows an example of the results. As can be seen, severe plastic deformation or elongation of the grains of the work material took place in the direction of cutting. The depth of cold-working measured in these tests is the same as that determined by the microhardness test.

6. Conclusion

This paper presents an energy based methodology for simulating the cutting force during the broaching operation. The mathematical formulation applied for the cutting force simulation is based on quantifying the contribution of different power components spent in the cutting system. The simulated cutting force and measured results are reasonably close; therefore, the proposed force model can be used for designing the broaching tool as well as optimizing the process. The depth of cold-working, which defines the distortions on heat treatment as well as the reliability of the parts, is a function of the uncut chip thickness and edge radius for standard broaching tool geometry. As such, the extent of the most severe plastic deformation is approximately 70 μm. This can be an accurate indicator in the selection of the proper radius of the cutting edge of the broaching tool as well as in the selection of the parameters of the subsequent heat treatment. Moreover, the modification of the shear flow stress of the work material due to cold-working is accounted in the force model.

Acknowledgements

The authors would like to acknowledge the support of the Natural Sciences and Engineering Research Council of Canada (NSERC). The authors also appreciate the assistance of Mr. Richard Blackwell, general manager of BUEHLER CANADA in performing surface integrity and microhardness tests.

References

[1] He G (1985) Experimental Investigations of the Surface Integrity of Broached Titanium Alloy. *Annals of the CIRP* 34(1):491–494.
[2] Konig W, Klinger R, Link R (1990) Machining Hard Materials with Geometrically Defined Cutting Edges-field of Applications and Limitations. *Annals of the CIRP* 39/1:61–64.
[3] Davim JP (2010) *Surface Integrity in Machining*, Springer.
[4] Ozlu E, Engin Ş, Cook C, El-Wardany T, Budak E (2010) Simulation of Broaching Operations for Tool Design Optimization. *Proceeding of the 2nd International CIRP Conference on Process Machine Interactions*, Vancouver, Canada.
[5] Astakhov VP, Xiao X (2008) A Methodology for Practical Cutting Force Evaluation Based on the Energy Spent in the Cutting System. *Machining Science and Technology* 12/3:325–347.
[6] Astakhov VP (2006) *Tribology of Metal Cutting*, Elsevier, London.
[7] Boresi AP, Schmidt RJ (2003) *Advanced Mechanics of Materials*, sixth ed. John Wiley & Sons, USA.
[8] Deutschman AD, Michels WA, Wilson CE (1975) *Machine Design Theory and Practice*, MacMillan Publishing.
[9] Yussefian NZ, Koshy P, Buchholz S, Klocke F (2010) Electro-erosion Edge Honing of Cutting Tools. *Annals of the CIRP* 59/1:215–218.